

Relation between the dark and photoelectronic properties of microcrystalline silicon

R. BRÜGGEMANN*, R.I. BADRAN^a, S. XIONG^b

Institut für Physik, Carl von Ossietzky Universität Oldenburg, D-26111 Oldenburg, Germany

^a *Physics Department, The Hashemite University, P.O. Box 150459, Zarqa, Jordan*

^b *Institute of Photo-electronics, Nankai University, Tianjin, 300071, China*

The dark conductivity, photoconductivity, and diffusion length have been determined in a comprehensive study on microcrystalline silicon samples, prepared under different deposition conditions: variation of substrate temperature, pressure, power, and silane to hydrogen ratio. The results show that the dark and majority carrier properties are correlated, which can be attributed to a Fermi-level related recombination rate and majority-carrier lifetime. In contrast, the observed distinct variation of the minority-carrier properties within a deposition series allows a more direct access to sample quality, as it cannot be directly linked with a Fermi level dependent lifetime. In contrast to the suggestion in the literature, the ratio of the mobility-lifetime products of both carrier types is shown not to be directly related to the Fermi level position.

(Received November 1, 2006; accepted December 21, 2006)

Keywords: Microcrystalline silicon, mobility-lifetime products, dark conductivity, photoconductivity

1. Introduction

Hydrogenated microcrystalline silicon ($\mu\text{c-Si:H}$) has been established as a material for photovoltaic applications [1-3]. For the photoelectronic characterisation of intrinsic layers for *pin* solar cells, the mobility-lifetime ($\mu\tau$) products in microcrystalline silicon ($\mu\text{c-Si:H}$) are important parameters, not only for reference to sample quality but also to reveal the underlying physics of recombination and transport and to construct a relation to the density of defects in the material. The experimental techniques for their determination are the steady-state photoconductivity (SSPC) for the majority-carrier $\mu\tau$ product ($\mu\tau$)_{maj} and the steady-state photocurrent grating technique (SSPG) [4] for the minority-carrier $\mu\tau$ product ($\mu\tau$)_{min}.

In the literature, the relation between photoconductivity, and thus majority-carrier $\mu\tau$ products, and dark conductivity has been discussed for hydrogenated amorphous silicon and $\mu\text{c-Si:H}$ [5,6 and references therein]. In this paper, we supply additional data sets on majority and minority carrier $\mu\tau$ products from a study on $\mu\text{c-Si:H}$ samples from different deposition series for which one deposition parameter was varied. We determine the $\mu\tau$ products and relate their values to the dark conductivity or Fermi level, and discuss the relation to the density of defects in the band gap.

2. Experimental

2.1. Sample details

Microcrystalline silicon samples were deposited by plasma-enhanced chemical vapour deposition (PECVD) at

Nankai University. The standard substrate temperature was 220 °C, standard power 25 W, standard pressure 120 Pa and standard hydrogen dilution 2 % silane in hydrogen in the gas flow. In addition to these standard parameters, different series were prepared with variations in pressure, substrate temperature, power or silane flow, while keeping the other parameters constant.

Coplanar Al electrodes were evaporated for electrical measurements. The crystalline volume fraction was determined from Raman spectra as a semi-quantitative measure of the crystalline volume fraction. All samples were stored in air for a couple of weeks before the photoconductive measurements.

2.2. Experimental details

All experiments were performed at room temperature in ambient air. We employed standard dark and steady-state photoconductivity measurements. The photocurrent I_{ph} and the mobility-lifetime product ($\mu\tau$)_{maj}, as determined from $\mu\tau = \sigma_{ph}/(eG)$, serve as an indicator of the majority-carrier properties. Here, σ_{ph} is the photoconductivity, e is the elementary charge, G is the mean photogeneration rate, for red-light illumination from a HeNe laser with a photon flux of about $10^{17} \text{ cm}^{-2} \text{ s}^{-1}$. We shall assume that the electron density n determines the photoconductivity, so that we equate the electron mobility-lifetime product ($\mu\tau$)_n to ($\mu\tau$)_{maj}.

For determination of the minority-carrier mobility-lifetime product, the SSPG technique [4] was applied. In the experiment, the diffusion length L_d was determined, from which ($\mu\tau$)_{min} was calculated by assuming it to be equal to ($\mu\tau$)_p. This assumption obviously implies that holes are the minority carriers.

3. Results

Fig. 1 shows the variation of the diffusion lengths that were determined by SSPG for various different deposition parameters. The other deposition parameters were kept constant, as described in section 2. There are clear correlations of the diffusion length with the parameters of pressure, power and deposition temperature.

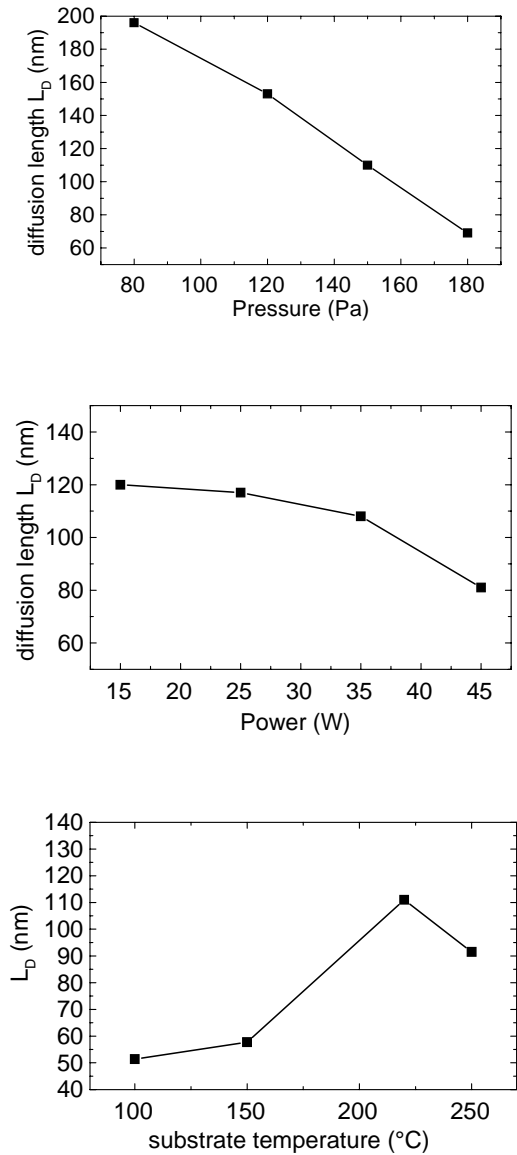


Fig. 1. Majority and minority carrier mobility-lifetime products $[(\mu\tau)_n \text{ and } (\mu\tau)_p]$ vs. dark conductivity, for those samples which exhibit a dark-conductivity value around $10^{-3} \Omega^{-1} \text{ cm}^{-1}$.

Fig. 2 gives an account of the diffusion lengths between 200 nm and 50 nm for most of the samples for which the dark conductivity is in a narrow range around $10^{-3} \Omega^{-1} \text{ cm}^{-1}$.

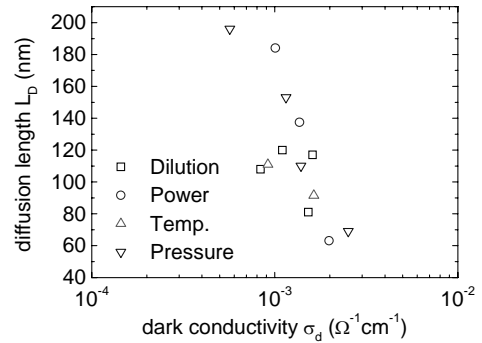


Fig. 2. Diffusion length vs. dark conductivity for the samples, indicating the variation in L_d with the longest L_d for low power and low pressure. The dark conductivity of most nominally undoped samples is large.

Fig. 3 summarises the majority and minority carrier mobility-lifetime products $[(\mu\tau)_n \text{ and } (\mu\tau)_p]$ as a function of dark conductivity, for all the samples. There is a larger number of data points at higher dark conductivities. Here, data show a much larger variation of $(\mu\tau)_p$ compared to $(\mu\tau)_n$. Note that for $(\mu\tau)_n$ there is also a larger tendency to drop with decreasing in dark conductivity.

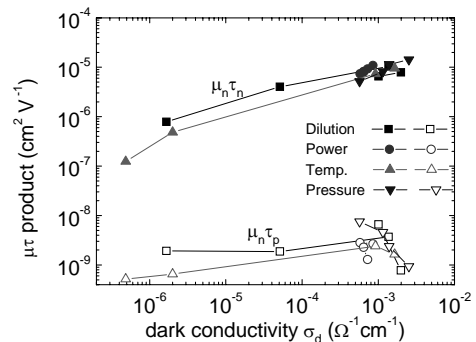


Fig. 3. Majority and minority carrier mobility-lifetime products $[(\mu\tau)_n \text{ and } (\mu\tau)_p]$ vs. dark conductivity. The upward triangles with low dark conductivity represent samples with deposition temperatures of 100 and 150 °C.

Fig. 4 relates the dark conductivity to the crystalline volume fraction. The line as a guide to the eye indicates the drop in dark conductivity as samples become more amorphous with decreasing of hydrogen dilution in the deposition gases. Two samples (upward triangles in Figs. 3 and 4) show both a high crystalline volume fraction and a low dark conductivity. For these, both mobility-lifetime products are low, indicating a high density of defects which may pin the Fermi level.

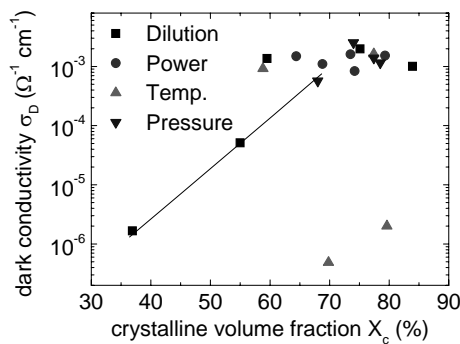


Fig. 4. Dark conductivity vs. crystalline volume fraction. The line is a guide to the eye. The upward triangles with low dark conductivity represent samples with deposition temperatures of 100 and 150 °C.

Fig. 5 shows the ratio of the mobility-lifetime products in terms of the parameter b [7-9], defined as $b = (\mu\tau)_n/(\mu\tau)_p$. Full symbols represent samples from the present series while open symbols are from different sets of microcrystalline silicon samples deposited by hot-wire chemical vapour deposition and PECVD. Most present samples exhibit higher dark conductivities than previously studied samples.

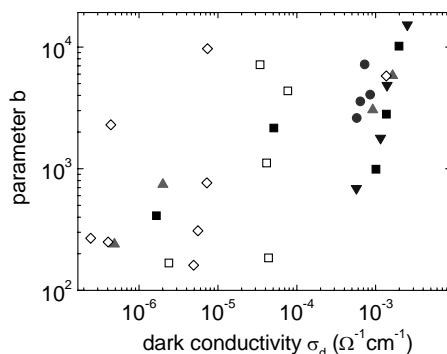


Fig. 5. Parameter b for the present samples (full symbols) and additional microcrystalline silicon samples (open symbols).

4. Discussion

Fig. 1 shows that the diffusion length as determined by SSPG gives useful information for sample characterisation and optimisation. Relying also on experience from previous studies [10,11], deposition regimes for the different series here that lead to short diffusion lengths and high defect densities can be identified. The summary in Figs. 3 and 4 shows that the dark conductivity of the samples with higher crystallinity is high. The variation in diffusion lengths in Fig. 2 or in the $(\mu\tau)_p$ products of Fig. 3 is larger than the corresponding variation in the $(\mu\tau)_n$ products. The latter is expected to also be influenced by the position of the Fermi level in the upper half of the

bandgap, which determines the occupation of defect levels and the electron capture and recombination times.

For the lower dark conductivity in Fig. 3, there is the often-observed drop in photoconductivity / $(\mu\tau)_n$ product as the Fermi level shifts further towards midgap [5,6]. High values of σ_{ph} are correlated here with high values of σ_d . The $(\mu\tau)_p$ product is not so much affected by the Fermi level shift. In Fig. 3 it is obvious though that this does not hold for the two samples with lower deposition temperature, for which the high crystalline volume fraction, the low dark-conductivity value and the low values of the $(\mu\tau)$ products indicate a high defect density.

The parameter b in Fig. 5 shows significant scatter when plotted vs. dark conductivity. For the present samples, most of the scatter in b reflects the variation in $(\mu\tau)_p$ compared to $(\mu\tau)_n$. Together with the b values for other microcrystalline silicon samples, for which the details about crystalline volume fraction and deposition conditions are not important in the present context, it is evident that there is no direct correlation between b and the dark conductivity or Fermi level. The results corroborate earlier analysis on a-Si:H samples [7] for which it was concluded that the dark conductivity is a better indicator of the Fermi level than the parameter b .

5. Conclusions

Photoconductive techniques like photoconductivity and SSPG are relatively simple for the determination of mobility-lifetime products. Photoconductivity data are more difficult to interpret, because the electron lifetime is related to and influenced by the Fermi level position so that the influence of the variation in defect density is masked. Minority carrier properties are less affected by Fermi level variation and are an indicator of the defect density in samples from the different deposition series. In particular, samples grown at high power and high pressure have a short diffusion length, which indicates a high defect density in these samples.

The parameter b shows significant scatter when plotted vs. dark conductivity, and has not been found to be linked with the Fermi level position in the microcrystalline silicon samples.

Acknowledgements

The authors thank S. Trotzky for measurements.

References

- [1] O. Vetterl, F. Finger, R. Carius, P. Hapke, L. Houben, O. Kluth, A. Lambertz, A. Mück, B. Rech, H. Wagner, Sol. Energy Mater. Sol. Cells **62**, 97 (2000).
- [2] J. Meier, E. Vallat-Sauvain, S. Dubail, U. Kroll, J. Dubail, S. Golay, L. Feitknecht, P. Torres, S. Fay, D. Fischer, A. Shah, Sol. Energy Mat. Sol. Cells **66**, 73 (2000).

- [3] S. Klein, J. Wolff, F. Finger, R. Carius, H. Wagner, M. Stutzmann, *Jpn. J. Appl. Phys. Part II: Letters* **41**, L10 (2002).
- [4] D. Ritter, E. Zeldov, K. Weiser, *Appl. Phys. Lett.* **49**, 791 (1986).
- [5] R. Brüggemann, *J. Mater. Sci. – Mater. Electron.* **14**, 629 (2003).
- [6] F. Finger, S. Klein, T. Dylla, A. L. Baia Neto, O. Vetterl, R. Carius, *MRS Symp. Proc.* **715**, A16.3 (2002).
- [7] R. Brüggemann, *Thin Solid Films* **427**, 355 (2003).
- [8] A. Shah, E. Sauvain, J. Hubin, C. Pipoz, C. Hof, *Philos. Mag. B* **75**, 925 (1997).
- [9] N. Beck, N. Wyrsh, C. Hof, A. Shah, *J. Appl. Phys.* **79**, 9361 (1996).
- [10] R. Brüggemann, *J. Optoelectron. Adv. Mater.* **7**, 495 (2005).
- [11] S. Okur, O. Gökta, M. Günes, F. Finger, R. Carius, *J. Optoelectron. Adv. Mater.* **7**, 191 (2005).

*Corresponding author: rudi.brueggemann@uni-oldenburg.de